ELSEVIER

Surface Science 462 (2000) 45–54

surface science

www.elsevier.nl/locate/susc

A scanning tunnelling microscopy view of the surfactant-assisted growth of iron on Cu(111)

M.C.G. Passeggi Jr. [a,*], J.E. Prieto [a], R. Miranda [a], J.M. Gallego [b]

[a] *Departamento de Física de la Materia Condensada, Universidad Autónoma de Madrid, Cantoblanco, 28049 Madrid, Spain*
[b] *Instituto de Ciencia de Materiales de Madrid–CSIC, Cantoblanco, 28049 Madrid, Spain*

Received 14 February 2000; accepted for publication 30 March 2000

Abstract

We report a scanning tunnelling microscopy study of the growth of iron on Cu(111) using lead as a surfactant. In the absence of surfactant, the growth of iron on Cu(111) proceeds in the form of three-dimensional islands, giving rise to an irregular granular film, with the presence of both face-centred cubic (fcc) and body-centred cubic crystallites whose relative population depends on the film thickness. The deposition of iron is accompanied by an active etching process, which results in chemical heterogeneity of the islands and the appearance of vacancy islands in the substrate surface. On the contrary, during the growth of iron on Pb/Cu(111): (1) the reaction at the interface is considerably limited, producing initially an almost perfect two-dimensional bilayer; (2) the subsequent growth results in a multi-level rough film due to limited interlayer mass transport; and (3) the iron film, continuous and monocrystalline, has the fcc structure as suggested by the persistence of a (4×4) lead superstructure present on the top surface layer up to at least six monolayers.

Keywords: Copper; Growth; Iron; Lead; Metallic films; Scanning tunneling microscopy; Surface structure, morphology, roughness, and topography

1. Introduction

It has been known for some time that the use of adsorbed gases [1] or metals [2] can improve the growth of thin metal films, changing the growth mode from a three-dimensional island growth (3D) to a two-dimensional layer-by-layer growth (2D), thus leading to smoother films. In metal-on-metal growth, the elements most commonly used have been antimony (Ag/Ag(111) [2], Co/Cu(111) [3]), oxygen (Cu/Ru(0001) [4], Pt/Pt(111) [5]), indium (Cu/Cu(111) [6], Ag/Ag(111) [7]) and lead (Cu/Cu(111) [8], Co/Cu(111) [9,10]). All of these elements, known as surfactants, have a lower free energy than the deposited metal [11], and tend to float during growth. The floating efficiency of lead seems to be particularly large, and indeed lead has been used for the growth of spin valve structures [12] and Co/Cu superlattices [13].

In this paper we explore the surfactant abilities of lead in another heteroepitaxial system, iron on Cu(111), with the ultimate purpose of growing face-centred cubic (fcc) iron films. Fcc iron is a fascinating material. It is known to have various magnetic structures depending on the lattice parameter [14], including paramagnetic, antiferromagnetic, ferromagnetic, low-moment ferromagnetic and high-moment ferromagnetic. However,

* Corresponding author. Fax: +34-91-397-3961.
E-mail address: mario.passeggi@uam.es (M.C.G. Passeggi Jr.)

0039-6028/00/$ - see front matter
PII: S0039-6028(00)00460-X

pure fcc films have proved difficult to prepare. A possible substrate for growing isotropic fcc iron is copper, due to the small lattice mismatch. While the growth of iron on Cu(100) produces different structures such as face-centred tetragonal (fct) [15], fcc [16] and body-centred cubic (bcc) [17], depending on the film thickness, with different magnetic properties [18], the thermal deposition of iron on Cu(111) at 300 K leads to a 3D island growth mode [19–21], with the iron clusters being either epitaxial bcc(110) or fcc(111) depending on the growth temperature and film thickness. At room temperature, the fcc-to-bcc transition proceeds between two and four monolayers (ML) as detected by low-energy electron diffraction (LEED) and X-ray photoelectron diffraction (XPD) [21,22]. On the other hand, pulsed laser deposition has been shown to yield flat films, probably pure fcc in the high-magnetic moment phase, but only for thicknesses below 6 ML [22].

As stated above, here we explore an alternative route to stabilize films of fcc iron on Cu(111), employing a lead surfactant layer. Auger electron spectroscopy (AES), LEED and scanning tunnelling microscopy (STM) results prove that use of the lead overlayer makes the iron film grow in a continuous and epitaxial manner, although from the third level on there is a substantially reduced interlayer mass transport and the film becomes rougher as the thickness increases. The threefold symmetric LEED pattern and the presence of the undistorted (4×4) lead overlayer suggest that the structure of the film is actually fcc, at least up to a coverage of ~ 6 ML.

2. Experimental set-up

The experiments were performed at room temperature in a ultrahigh vacuum (UHV) chamber equipped with a home-made STM unit described elsewhere [23] and a rear-view, four-grid LEED optics, which was also used to acquire Auger electron spectra. The sample holder allowed in situ transfer from the LEED optics to the STM head. The substrate was a Cu(111) single crystal mechanically polished and cleaned by cycles of Ar^+ ion bombardment (500 V) at room temperature followed by annealing at 850 K until no contamination was present in the AES spectrum. The LEED pattern of this surface presented the expected (1×1) threefold symmetry characteristic of the (111) face of the fcc substrate. Deposition of lead and iron was carried out by evaporation from lead and iron dispensers heated by electron bombardment, with the sample kept at room temperature. For low coverages, the deposition rate was calibrated by measuring the fraction of covered surface in the STM images. Larger coverages were deduced from the evaporation time and cross-checked by the ratios of the low- and high-energy Auger peaks of iron and lead with respect to that of copper. Considering the uncertainties involved, the error in the coverage has been estimated to be around 20%. The STM tip was a chemically etched, polycrystalline tungsten wire. The piezodrives were calibrated vertically by measuring the step height on the clean Cu(111) surface, and laterally by measuring the nearest-neighbour distance in images with atomic resolution.

3. Results

It is well known that, at room temperature, the growth of lead on Cu(111) takes place in the Stranski–Krastanov mode [24,25]. For coverages below 0.4 ML, a surface alloy is formed as lead atoms are incorporated into the Cu(111) surface [26]. Further deposition leads to dealloying and eventually, for coverages near 1 ML, to the formation of a close-packed lead overlayer with an incommensurate (4×4) superstructure. For larger coverages, three-dimensional crystalline clusters of lead are formed. In Fig. 1 we show the LEED pattern taken after depositing a lead coverage slightly above 1 ML on the clean Cu(111) surface (Fig. 1d). A (4×4) LEED superstructure with sharp spots and low background can be clearly observed.

As proved in Fig. 1, the lead layer floats very efficiently during the growth of iron on Cu(111) while retaining the (4×4) symmetry, just as in the growth of copper or cobalt on Cu(111) [8,9]. Fig. 1a shows two low-energy Auger spectra superimposed. The first one (solid line) corresponds to an overlayer of lead deposited on the Cu(111)

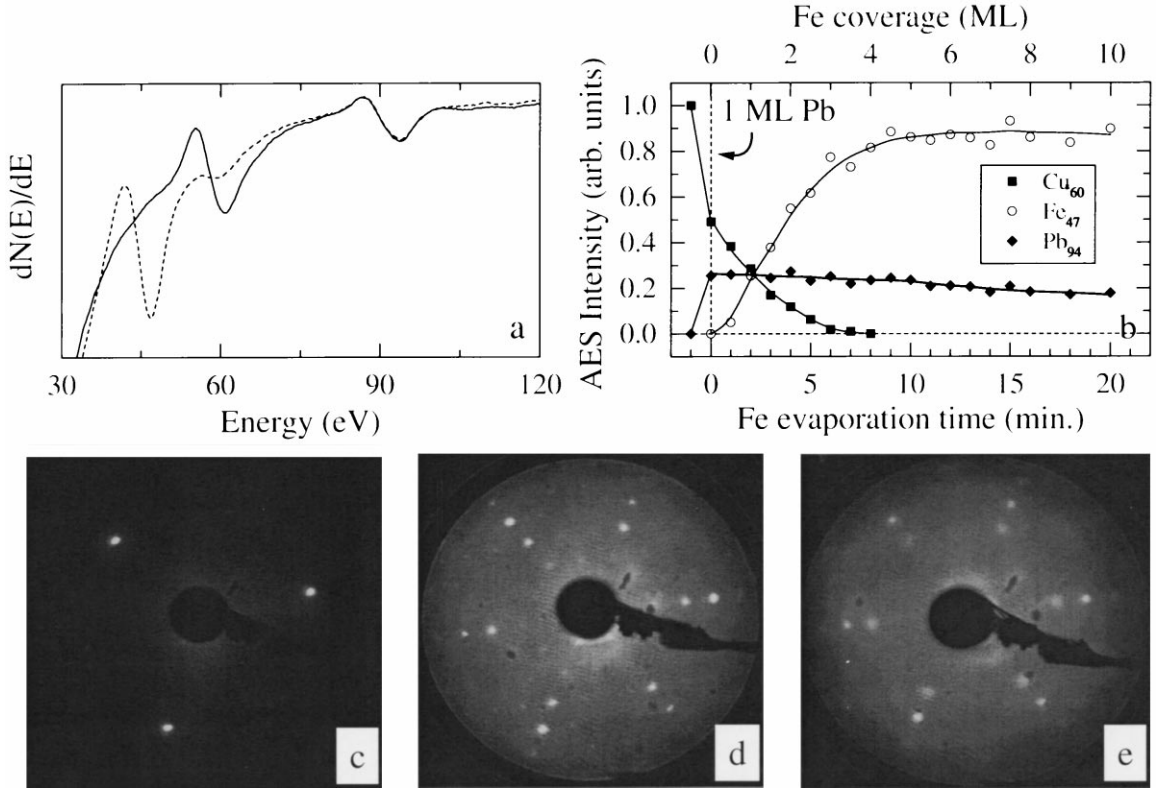

Fig. 1. (a) Low-energy Auger spectra taken after depositing ~1 ML of lead on Cu(111) (solid line) and after depositing ~4 ML of iron on Pb/Cu(111) (dotted line); (b) evolution of the Cu_{60}, Fe_{47} and Pb_{94} Auger intensities during the deposition of iron on Pb/Cu(111); (c) LEED pattern of the clean Cu(111) surface; (d) after depositing 1 ML of lead on Cu(111); and (e) after depositing ~7.0 ML of iron on Pb/Cu(111).

surface, showing the low-energy Cu_{61} and Pb_{92} Auger transitions. The second spectrum (dashed line) was acquired after depositing a ~4 ML thick film of iron on the Pb/Cu(111) interface. From this spectrum it is obvious that the iron film produces the almost complete disappearance of the substrate signal at 61 eV. Instead, an iron-related Auger peak appears at 47 eV. Thus the iron film has covered totally the substrate and its thickness is enough to make the low-energy copper signal disappear. On the other hand, the lead signal shows only a negligible decrease in intensity during the iron evaporation process. Thus, the low-energy Auger spectra demonstrate that the lead layer floats over the iron film, which, in turn, covers the Cu(111) substrate. This is also confirmed by the evolution of the peak-to-peak amplitudes of the Auger Fe_{47}, Cu_{61} and Pb_{92} transitions versus iron evaporation time (Fig. 1b). While the copper Auger signal decreases and the iron signal increases as expected, the lead intensity remains almost constant, displaying only a very small decrease along the whole process. Fig. 1 also reproduces the LEED patterns measured on the clean Cu(111) surface (Fig. 1c), after depositing 1 ML of lead (Fig. 1d) and after evaporating a thick film of iron (~7.0 ML) on the Pb/Cu(111) interface (Fig. 1e). For comparison purposes the patterns have been acquired at the same electron kinetic energy (135 eV). The clean copper surface presents the expected (1×1) threefold symmetry. As we have already pointed out, the lead overlayer deposited on the clean Cu(111) surface shows a (4×4) symmetry pattern, which is also observed after the

thick iron film has been deposited, although giving less intense diffraction spots and some more background. These last two observations indicate that the size of the lead (4×4) ordered areas have diminished due to island formation in the iron film. Otherwise, the (4×4) symmetry of the diffraction pattern is still present. The LEED results clearly confirm the AES observations; i.e., the lead overlayer segregates to the outer surface of the iron film, maintaining the (4×4) structure over the iron layers. Since the (4×4) lead superstructure has been observed only for growth on substrates with hexagonal surfaces, such as fcc Cu(111) [27] and Ni(111) [28] or hcp Co(0001) [29], and the LEED pattern shows a clear threefold symmetry up to coverages near $\sim$6.0 ML, it is very likely that the iron layers have the fcc structure.

Fig. 2 shows STM images of 0.25 ML of iron on Cu(111) deposited at a rate of 0.5 ML min^{-1}. The image in Fig. 2a was taken after evaporation on the clean surface, i.e., without a predeposited lead layer. As previously reported [19,20,30], iron deposition produces the formation of three-dimensional islands, with an approximately hexagonal shape and mostly bilayer-high, although the top surface of the islands is rather rough, with height values ranging between 4 and 5.5 Å. A typical profile scan acquired across one of the islands of Fig. 2a is shown in Fig. 2c. The characteristic lateral size of the islands is $\sim$100 Å. All of the steps in the images appear to be decorated with islands 1–2 ML high. Also, after the evaporation of iron, a number of 2 Å deep holes (i.e., vacancy islands) appear on the copper terraces (one of them is marked with an arrow in Fig. 2a). Similar observations have been reported for cobalt on Cu(111) [31,32]. These two processes, decoration

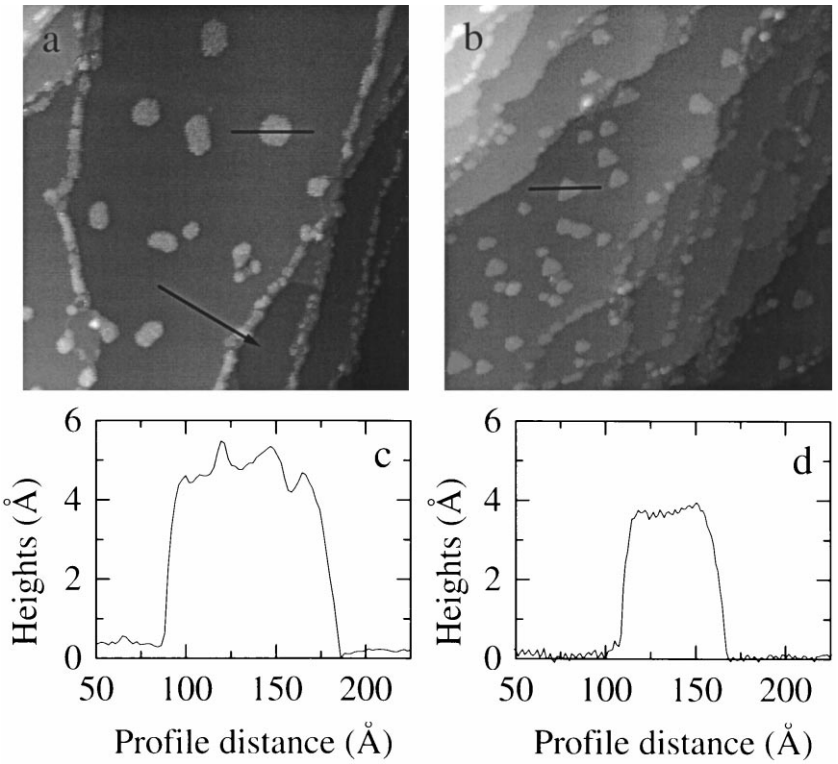

Fig. 2. STM images (1000 Å × 1000 Å) taken after depositing 0.25 ML of iron at 300 K on the (a) clean Cu(111) surface and (b) the Cu(111) surface where 1 ML of lead has been predeposited; (c) and (d) profile scans acquired across the islands marked in (a) and (b), respectively. The arrow in (a) points to a large vacancy island on a terrace of the copper surface.

of steps and formation of holes, seem to be related, and a strain-driven mechanism has been proposed for this iron-induced copper diffusion process [30].

The STM image reproduced in Fig. 2b was taken after depositing 0.25 ML of iron on the Cu(111) surface precovered with 1 ML of lead. Although the size of the terraces is not large enough to provide a reliable quantitative description, the density of islands is significantly higher than without lead, indicating a decrease in the effective diffusion coefficient of the mobile atoms. The islands, with an average lateral size of 50 Å, are bilayer-high. Probably due to electronic effects, the measured heights depend somewhat on the tunnelling conditions, and no unique number can be given. The most common values range between 3.6 and 4.0 Å. Nevertheless, their top surface is smoother in this case as demonstrated in the profile scan of Fig. 2d. Note also that, in general, the shape of the islands is triangular rather than hexagonal and more regular. Just as without lead, the steps appear decorated by islands. However, no holes were observed on the surface of the copper substrate. Atomic-resolution pictures (not shown here) prove the presence of the (4×4) lead overlayer on top of the islands, as well as on the substrate surface.

We show in Fig. 3 typical STM images for a coverage of 1.3 ML of iron, deposited at a rate of 0.5 ML min^{-1}, without (Fig. 3a) and with (Fig. 3b) lead. Note that, while the islands in Fig. 3a are either two or three layers high, in Fig. 3b most of them are two layers high with only a small fraction of the third level present. This suggests the existence of different atomic processes controlling the growth morphology in both cases. Without lead, in order to have the third level completely occupied in many islands, there must have been a significant amount of upwards diffusion within the islands. On the other hand, with lead, this upwards current seems to be limited to the second level. The amount of material in the third level could be explained by the number of iron atoms that have landed on top of the two-level islands. The most significant difference between the two cases, however, lies in the regularity and smoothness of the islands when lead has been predeposited. Without lead (Fig. 3a) there are triangular and hexagonal islands with a rather irregular shape, but with lead (Fig. 3b) the shape of the islands is always triangular and much more regular. This is different from the case of cobalt deposited on Pb/Cu(111) [29]. Another important difference with the case of cobalt lies in the chemical homogeneity of the islands prepared without or with surfactant. In the first case, the short-range roughness of the surface and its irregular morphology, which prevent the acquisition of atomic-resolution images on top of the islands, seem to imply a heterogeneous composition, with some copper atoms intermixed within the iron islands. On the contrary, when lead is used, the top surface is very flat and the (4×4) lead overlayer looks undistorted,

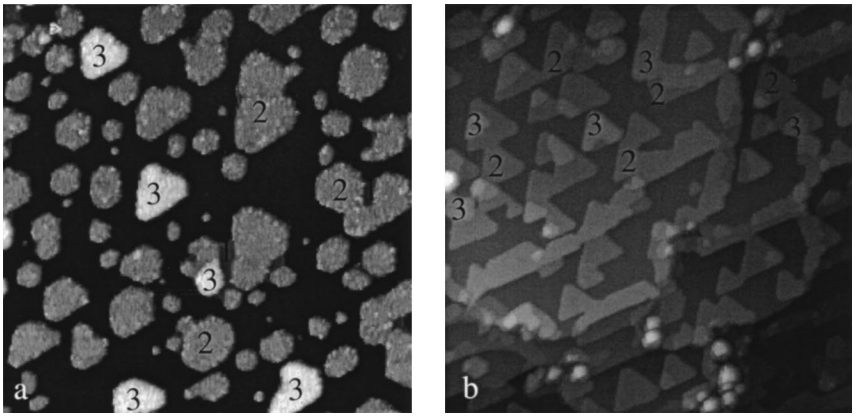

Fig. 3. STM images (1000 Å × 1000 Å) taken after evaporating ~1.3 ML of iron at 300 K on (a) the clean Cu(111) surface and (b) the Cu(111) surface where 1 ML of lead has been predeposited. The numbers indicate the number of layers above the substrate.

which point to a rather homogeneous composition. Note also that with lead, all of the islands are oriented in the same direction.

If, up to this coverage, the most significant difference between the iron films grown with and without lead seems to be limited to the growth of more regular (in shape and height) two-layer-high islands, the influence of the predeposited lead layer becomes more evident near the completion of the first bilayer. Fig. 4 presents STM images taken after evaporating ~2.0 ML of iron. Without lead (Fig. 4a), ~50% of the substrate surface still remains uncovered. With respect to the images in Fig. 3a, the 3D islands have increased in height, reaching 8–10 Å, but their density and lateral size remain approximately constant. Although the top surface of the islands is still very rough, there seems to be a coexistence of three-, four- and five-level islands, the mean value being 8 Å (i.e., four levels). This can be observed in Fig. 4c, where we reproduce the island heights obtained along the profile scan shown in Fig. 4a. All of these features constitute a clear indication of a 3D growth mode.

Predeposition of the lead monolayer changes the scenario completely. In this case (Fig. 4b) the bilayer is almost completed, while the population of the third level has not increased significantly. The fact that the islands share the same orientation and coalesce in a smooth way, leaving no empty space between them, imply that they must have nucleated in equivalent sites of the copper surface, following the stacking sequence of the substrate. Thus, the surface retains a two-dimensional character. In Fig. 4d we show a profile scan that demonstrates a drastically reduced surface roughness due to the presence of the surfactant (compare with Fig. 4c).

For the clean surface, when the iron coverage

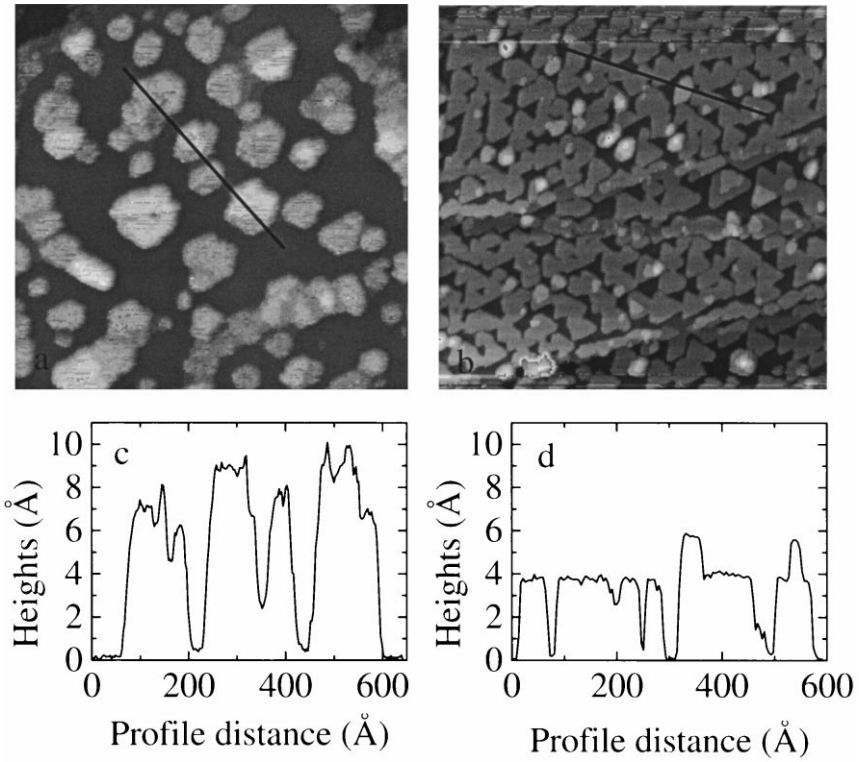

Fig. 4. STM images (1000 Å × 1000 Å) taken after evaporating ~2.0 ML of iron at 300 K on (a) the clean Cu(111) surface and (b) the Cu(111) surface where 1 ML of lead has been predeposited; (c) and (d) profile scans across the islands shown in (a) and (b), respectively.

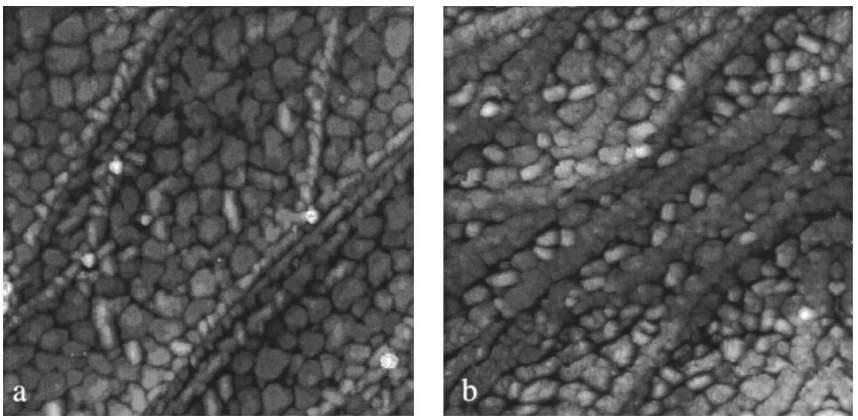

Fig. 5. STM images (2000 Å × 2000 Å) taken after evaporating (a) ~3.5 ML and (b) ~7.0 ML of iron on the clean Cu(111) surface.

increases to ~3.5 ML (Fig. 5a), the islands grow in height and lateral size until they cover the substrate surface almost completely. In this case, however, the islands do not coalesce easily, and the individual grains can still be distinguished. Note already in Fig. 5a the presence of some elongated ridge-like structures. These have been recognized as bcc(110) precipitates with the Kurdjumov–Sachs orientation with respect to the fcc substrate [22]. For larger coverages (Fig. 5b, ~7.0 ML) these bcc crystallites dominate the surface morphology, and the characteristic LEED pattern corresponding to the growth of bcc Fe(110) on Cu(111) with six equivalent domains can be observed (not shown here). Up to this point the film morphology retains the granular structure. On the contrary, on the lead-precovered surface, the first two monloayers of iron grow as a continuous, almost perfect, two-dimensional film. From there on, however, the growth proceeds in a multi-level way, although the film is still continuous; that is, the individual islands coalesce without leaving empty voids as the different levels are being completed. Fig. 6a shows a typical image of the surface after depositing ~2.9 ML of iron on the Pb/Cu(111) surface. In this case the initial bilayer is almost completely occupied (98%) while the third level is more than 60% filled. Note,

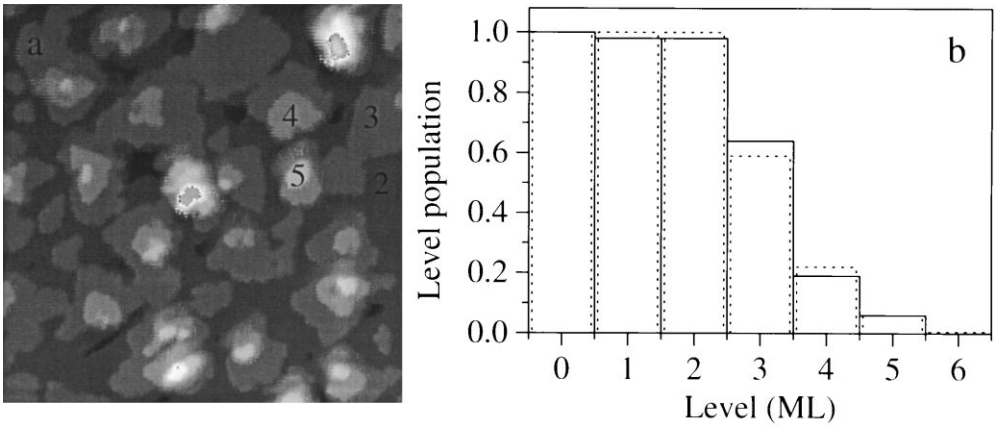

Fig. 6. (a) STM image (500 Å × 500 Å) taken after evaporating ~2.9 ML of iron on the Pb/Cu(111) surface; (b) population of the different levels observed in the image shown in (a). The dotted line corresponds to a Poisson distribution of levels on top of a perfect bilayer.

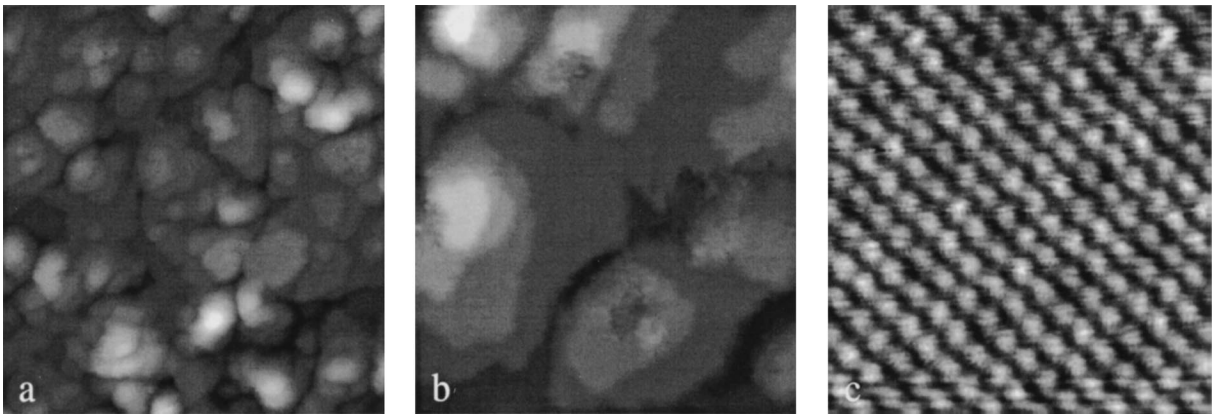

Fig. 7. STM images taken after evaporating ~7.0 ML of iron on the Pb/Cu(111) surface: (a) 500 Å × 500 Å; (b) 200 Å × 200 Å; (c) 45 Å × 45 Å.

however, that the fourth level has started to populate well before completion of the third level, and there is already a non-negligible occupation of the fifth level in some islands. The measured level population is shown in Fig. 6b as a solid line, while the dotted line represents a Poisson distribution of levels on top of a complete bilayer. The agreement is very good, which implies the existence of a substantially reduced interlayer mass transport from the third level on. In this way the number of exposed levels increases quickly with the iron coverage (for a Poisson distribution the growth front $\omega \sim \sqrt{\theta}$), but even after depositing 7.0 ML of iron (Fig. 7) the top surface of each level is rather flat, and the (4×4) lead superstructure can be resolved on all of them (see, for instance, Fig. 7c).

4. Discussion

The surface free energies of iron and copper are $\gamma_{Fe} = 2.939$ and $\gamma_{Cu} = 1.934$ J m^{-2} [11], respectively. Thus $\Delta\gamma = \gamma_{Cu} - (\gamma_{CuFe} + \gamma_{Fe}) \sim -1$ J m^{-2}, a rather large negative number (the interface free energies usually are small numbers), which explains the 3D growth mode of iron on Cu(111). The presence of the lead layer, with a low surface free energy ($\gamma_{Pb} = 0.534$ J m^{-2}), avoids this problem since in this case the energy balance $\Delta\gamma = (\gamma_{CuPb} + \gamma_{Pb}) - (\gamma_{CuFe} + \gamma_{FePb} + \gamma_{Pb})$ turns out to be a much smaller number than without lead.

Thus, the predeposition of 1 ML of lead changes the wetting of iron on Cu(111), producing a continuous and smoother (although multi-level) film instead of a 3D granular film. At low iron coverages, the lead overlayer causes a decrease in the effective diffusion coefficient of the iron atoms, as proved by the higher island density. At the same time, the islands, two layers high, are more regular in shape, height and orientation, and seem to be nucleated at equivalent sites of the copper surface, preventing the formation of twins and stacking faults at the interface. In addition, once the bilayer islands are formed, the lead overlayer must forbid, probably due to kinetic reasons, the upwards diffusion current of the new atoms that arrive to the islands, which thus grow in lateral size instead of height until they form a continuous, flat iron film. Further iron deposition makes the islands to coalesce, forming an almost perfect continuous bilayer, whereupon the growth proceeds in a multi-level way due to the absence of interlayer mass transport between the iron layers. In this way, the surfactant effect of lead is very effective in stopping the agglomeration and interfacial reactions during the growth of iron on Cu(111) but seems to be not enough to extend the layer-by-layer growth into the iron on Fe(111) regime.

This surfactant behaviour is very different from that observed in the room-temperature growth of copper and cobalt on Cu(111). In these systems,

interlayer mass transport seems to be hindered by the existence of an energy barrier for downwards diffusion over a step edge (the so-called Ehrlich–Schwoebel barrier) [33,34], but the presence of the lead layer makes the films grow layer-by-layer [8,10,29]. Although the general mechanisms for the surfactant action remain unclear [5,35–39], it has been recently proposed that, for the case of copper on Cu(111) [8], the presence of the lead layer changes the microscopic mechanism of diffusion. Instead of moving by hopping on the terraces, now the deposited atoms exchange place quickly with the lead atoms of the surfactant layer and then diffuse underneath the lead layer by making further exchanges with copper atoms from the substrate. In this way the energy barrier for diffusion along terraces, E_{surf}, increases considerably with respect to the clean deposition. Therefore, the *additional* activation barrier $\Delta E = E_{step} - E_{surf}$ for the downward hopping of an adatom over the island edges is effectively reduced, and the interlayer diffusion becomes as efficient as the intralayer one.

For obvious reasons, there are no experimental data regarding the growth of iron on fcc Fe(111). Therefore, the actual size of the Ehrlich–Schwoebel barrier is not known. From the behaviour of similar systems one can expect that it will exist and be large. From our data it is clear that, even with the lead layer, there is no easy downwards diffusion of the iron atoms. Thus, although the diffusion on the terraces is slowed by the presence of the lead layer, the value of the Ehrlich–Schwoebel barrier even with lead seems to be large enough to prevent interlayer diffusion.

To conclude, the behaviour described here for the growth of iron on lead-precovered Cu(111) is so different from that observed for cobalt and copper deposition on the same system that it must be rooted in some substantial difference in the prevalent diffusion processes for iron and cobalt (or copper), respectively, on the lead-covered Cu(111) surface.

Concerning the crystalline structure of the iron films prepared with the surfactant, the regularity of the islands at low coverages and their common orientation with respect to the substrate seem to indicate that they follow the fcc stacking of the substrate, forming a continuous, monocrystalline fcc iron film. For larger coverages, the presence of the (4×4) lead overlayer is consistent with the existence of a hexagonal close-packed layer underneath, which further supports the assumption of an fcc, (111)-oriented, iron film. Preliminary LEED I–V measurements, which show a clear threefold symmetry, confirm these assumptions.

Acknowledgements

We thank Dr. Vázquez de Parga for help during the initial setting-up of the experimental system. This work was partially supported by the Spanish CICyT (under grants MAT98-0965-C0401 and MAT98-0965-C0402) and DGES (under grant PB97-0031) and the Argentinian Fundación Antorchas (under grant A-13564/1-30). One of us (M.C.G.P.) thanks the Comisión Interministerial de Ciencia y Tecnología (Spain) for financial support, and CONICET (Argentina) for a fellowship.

References

[1] W.F. Egelhoff Jr., D.A. Steigerwald, J. Vac. Sci. Technol. A 7 (1989) 2167.
[2] H.A. van der Vegt, H.M. van Pinxteren, M. Lohmeier, E. Vlieg, J.M.C. Thornton, Phys. Rev. Lett. 68 (1992) 3335.
[3] V. Scheuch, K. Potthast, B. Voigtländer, H.P. Bonzel, Surf. Sci. 318 (1994) 115.
[4] M. Schmidt, H. Wolter, M. Nohlen, K. Wandelt, J. Vac. Sci. Technol. A 12 (1994) 1818.
[5] S. Esch, M. Hohage, T. Michely, G. Comsa, Phys. Rev. Lett. 72 (1994) 518.
[6] H.A. van der Vegt, J. Alvarez, X. Torrelles, S. Ferrer, E. Vlieg, Phys. Rev. B 52 (1995) 17443.
[7] H.A. van der Vegt, W.J. Huisman, P.B. Howes, T.S. Turner, E. Vlieg, Surf. Sci. 365 (1996) 205.
[8] J. Camarero, J. Ferrón, V. Cros, L. Gómez, A.L. Vázquez de Parga, J.M. Gallego, J.E. Prieto, J.J. de Miguel, R. Miranda, Phys. Rev. Lett. 81 (1998) 850.
[9] J. Camarero, L. Spendeler, G. Schmidt, K. Heinz, J.J. de Miguel, R. Miranda, Phys. Rev. Lett. 73 (1994) 2448.
[10] J. Camarero, T. Graf, J.J de Miguel, R. Miranda, W. Kuch, M. Zharnikov, A. Dittschar, C.M. Schneider, J. Kirschner, Phys. Rev. Lett. 76 (1996) 4428.
[11] Z. Mezey, J. Giber, Jpn. J. Appl. Phys. 21 (1982) 1569.
[12] W.F. Egelhoff Jr., P.J. Chen, C.J. Powell, M.D. Stiles, R.D.

McMichael, C.-L. Lin, J.M. Sivertsen, J.H. Judy, K. Takano, A.E. Berkowitz, J. Appl. Phys. 80 (1996) 5183.
[13] J. Camarero, V. Cros, M.J. Capitán, J. Álvarez, S. Ferrer, M.A. Niño, J.E. Prieto, L. Gómez, J. Ferrón, A.L. Vázquez de Parga, J.M. Gallego, J.J. de Miguel, R. Miranda, Appl. Phys. A 69 (1999) 553.
[14] V.L. Moruzzi, P.M. Marcus, J. Kübler, Phys. Rev. B 39 (1989) 6957.
[15] S.H. Lu, J. Quinn, D. Tian, F. Jona, P.M. Marcus, Surf. Sci. 209 (1989) 364.
[16] M.F. Onellion, C.L. Fun, M.A. Thompson, J.L. Erskine, A.J. Freeman, Phys. Rev. B 33 (1986) 7322.
[17] D. Pescia, M. Stampanoni, G.L. Bona, A. Vaterlaus, R.F. Willis, F. Meier, Phys. Rev. Lett. 58 (1987) 2126.
[18] S. Müller, P. Bayer, C. Reischl, K. Heinz, B. Feldmann, H. Zillgen, M. Wutting, Phys. Rev. Lett. 74 (1995) 765.
[19] A. Brodde, H. Neddermeyer, Ultramicroscopy 42–44 (1992) 556.
[20] A. Brodde, K. Dreps, J. Binder, Ch. Lunau, H. Neddermeyer, Phys. Rev. B 47 (1993) 6609.
[21] M.T. Kief, W.F. Egelhoff Jr., Phys. Rev. B 47 (1993) 10785.
[22] J. Shen, P. Ohresser, Ch.V. Mohan, M. Klaua, J. Barthel, J. Kirschner, Phys. Rev. Lett. 80 (1998) 1980.
[23] D.M. Zeglinski, D.F. Ogletree, T.P. Beebe Jr., R.Q. Hwang, G.A. Somorjai, M.B. Salmerón, Rev. Sci. Instrum. 61 (1990) 3769.
[24] C. Ocal, E. Martínez, S. Ferrer, Surf. Sci. 136 (1984) 571.
[25] G. Meyer, M. Michailov, M. Henzler, Surf. Sci. 202 (1988) 125.
[26] C. Nagl, O. Haller, E. Platzgummer, M. Schmid, P. Varga, Surf. Sci. 321 (1994) 237.
[27] J. Henrion, G.E. Rhead, Surf. Sci. 29 (1972) 20.
[28] K. Umezawa, A. Takahashi, T. Yumura, S. Nakanishi, W.M. Gibson, Surf. Sci. 365 (1996) 118.
[29] J.E. Prieto, Ch. Rath, S. Müller, L. Hammer, K. Heinz, R. Miranda, Phys. Rev. B, submitted for publication.
[30] M. Klaua, H. Höche, H. Jenniches, J. Barthel, J. Kirschner, Surf. Sci. 381 (1997) 106.
[31] J. de la Figuera, J.E. Prieto, C. Ocal, R. Miranda, Phys. Rev. B 47 (1993) 13043.
[32] J. de la Figuera, J.E. Prieto, C. Ocal, R. Miranda, Surf. Sci. 307–309 (1994) 538.
[33] W. Wulfhekel, N.N Lipkin, J. Kliewer, G. Rosenfeld, L.C. Jorritsma, B. Poelsema, G. Comsa, Surf. Sci. 348 (1996) 227.
[34] J. de la Figuera, J.E. Prieto, G. Kostka, S. Müller, C. Ocal, R. Miranda, K. Heinz, Surf. Sci. 349 (1996) L139.
[35] G. Rosenfeld, R. Servaty, C. Teichert, B. Poelsema, G. Comsa, Phys. Rev. Lett. 71 (1993) 895.
[36] I. Markov, Phys. Rev. B 50 (1994) 11271.
[37] Z.Z. Zhang, M.G. Lagally, Phys. Rev. Lett. 72 (1994) 693.
[38] J. Vrijmoeth, H.A. van der Vegt, J.A. Meyer, E. Vlieg, R.J. Behm, Phys. Rev. Lett. 72 (1994) 3843.
[39] N. Memmel, E. Bertel, Phys. Rev. Lett. 75 (1995) 485.